

# CHEMISTRY

## A European Journal

A Journal of



### Accepted Article

**Title:** Three-component Activation–Alkynylation–Cyclocondensation (AACC) Synthesis of Enhanced Emission Solvatochromic 3-Ethynyl Quinoxalines

**Authors:** Thomas J. J. Müller, Franziska K. Merkt, Simon P. Höwedes, Charlotte F. Gers-Panther, Irina Gruber, and Christoph Janiak

This manuscript has been accepted after peer review and appears as an Accepted Article online prior to editing, proofing, and formal publication of the final Version of Record (VoR). This work is currently citable by using the Digital Object Identifier (DOI) given below. The VoR will be published online in Early View as soon as possible and may be different to this Accepted Article as a result of editing. Readers should obtain the VoR from the journal website shown below when it is published to ensure accuracy of information. The authors are responsible for the content of this Accepted Article.

**To be cited as:** *Chem. Eur. J.* 10.1002/chem.201800079

**Link to VoR:** <http://dx.doi.org/10.1002/chem.201800079>

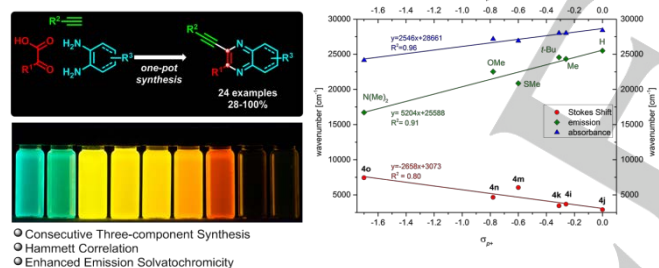
Supported by  
**ACES**

WILEY-VCH

# Three-component Activation–Alkynylation–Cyclocondensation (AACC) Synthesis of Enhanced Emission Solvatochromic 3-Ethynyl Quinoxalines

Franziska K. Merkt,<sup>a</sup> Simon P. Höwedes,<sup>a</sup> Charlotte F. Gers-Panther,<sup>a</sup> Irina Gruber,<sup>b</sup> Christoph Janiak,<sup>b</sup> and Thomas J. J. Müller<sup>\*,a</sup>

**Abstract:** 2-Substituted 3-ethynyl quinoxaline chromophores can be readily synthesized by a consecutive activation–alkynylation–cyclocondensation (AACC) one-pot sequence in a three-component fashion. In comparison to the previously published four-component glyoxylation starting from electron rich  $\pi$ -nucleophiles, the direct activation of (hetero)aryl glyoxylic acids allows introducing substituents that cannot be directly accessed by glyoxylation. By introduction of *N,N*-dimethyl aniline as a strong donor in position 2 the emission solvatochromicity of 3-ethynyl quinoxalines can be considerably enhanced, covering the spectral range from bluegreen to deep red orange with a single chromophore in a relatively narrow polarity window. The diversity-oriented nature of the synthetic multicomponent reaction concept furthermore enables comprehensive investigations of structure-property relationships by Hammett correlations and Lippert-Mataga analysis, as well as the elucidation of the electronic structure of the emission solvatochromic  $\pi$ -conjugated donor-acceptor systems by DFT and TD-DFT calculations employing the PBEh1PBE functional for a better reproduction of the dominant charge transfer character of the longest wavelength absorption band.



## Introduction

Tailor-made fluorophores with designed emission characteristics have become increasingly important as functional constituents<sup>[1]</sup> in materials and life sciences and their applications are wide spread, from organic electronics,<sup>[2]</sup> such as OFET (organic field effect transistors), OLED (organic light emitting diodes), and

DSSC (dye sensitized solar cells),<sup>[3]</sup> to bioanalytical imaging and sensing,<sup>[4]</sup> and diagnostics.<sup>[5]</sup> Fluorophores with color response to the surrounding media are particularly interesting.<sup>[6]</sup> This phenomenon observable by eye-sight is called solvatochromism<sup>[7]</sup> and it directly corresponds to significant change of the dipole moment upon excitation of the chromophore from  $S_0$  to the vibrationally relaxed  $S_1$  state.<sup>[8]</sup> As a consequence a steady demand for novel fluorophore structures and emission profiles poses a major challenge to synthetic chemistry, which provides suitable libraries for systematic investigations establishing reliable structure-property correlations of the photophysical behavior. Diversity-oriented synthesis<sup>[9]</sup> is very advantageous, since highly diverse products can be readily obtained by the same reaction principle through variation of suitable starting materials. In particular, multicomponent reactions (MCR)<sup>[10]</sup> and one-pot strategies combine beneficial economic and ecological aspects for reaching this challenging goal. In the sense of a chromophore concept, a chromogenic application of the MCR concept, functional chromophores have become accessible more easily and more generally,<sup>[11]</sup> an approach that has now been systematically extended to a powerful tool in fluorophore design.<sup>[12]</sup>

Quinoxaline and pyrazine dyes, which can be designed by various strategies,<sup>[13]</sup> have received considerable attention as most prospective and potential electroluminescent materials<sup>[14-17]</sup> and as functional chromophores in bioanalytics.<sup>[18,19]</sup> These electron withdrawing core heterocycles represent a unit of paramount importance for the construction of push-pull systems<sup>[20,21]</sup> and intramolecular charge-transfer complexes (ICT).<sup>[22]</sup> The presence of the Brønsted and Lewis basic nitrogen atoms<sup>[23]</sup> promises furthermore emission sensitivity towards changes in the surrounding medium triggered by pH, metal ions, solvent polarity or biological analytes.<sup>[24,25]</sup> Besides their luminescence, they also display pronounced solvatochromic shifts of the emission bands. Solvatochromic quinoxaline-based push-pull systems were employed as emissive probes for the binding-site polarity of bovine serum albumin,<sup>[26]</sup> for exploring site-dependent fluorescence in HEp-2 cells,<sup>[27]</sup> and as chromophores for dye-sensitized solar cells.<sup>[28]</sup> Only recently, we<sup>[27,29]</sup> and Jiang<sup>[30]</sup> described the synthesis of emission-solvatochromic indole-substituted quinoxaline derivatives.

In particular, we employed a glyoxylation-alkynylation-cyclocondensation (GACC) sequence for accessing 3-ethynyl quinoxalines in the sense of a consecutive four-component reaction, and as an extension by concatenating a concluding Michael addition a glyoxylation-alkynylation-cyclocondensation-addition (GACCA) sequence for accessing 3-( $\beta$ -aminovinyl) quinoxalines in the sense of a consecutive five-component reaction evolved (Figure 1).

[a] M. Sc. Franziska K. Merkt, B. Sc. Simon P. Höwedes, Dr. Charlotte F. Gers-Panther, Prof. Dr. Thomas J. J. Müller  
Institut für Organische Chemie und Makromolekulare Chemie  
Heinrich-Heine-Universität Düsseldorf  
Universitätsstraße 1, D-40225 Düsseldorf, Germany.  
E-mail: ThomasJJ.Mueller@uni-duesseldorf.de

[b] M. Sc. Irina Gruber, Prof. Dr. Christoph Janiak  
Institut für Anorganische Chemie und Strukturchemie  
Heinrich-Heine-Universität Düsseldorf  
Universitätsstraße 1, D-40225 Düsseldorf, Germany.

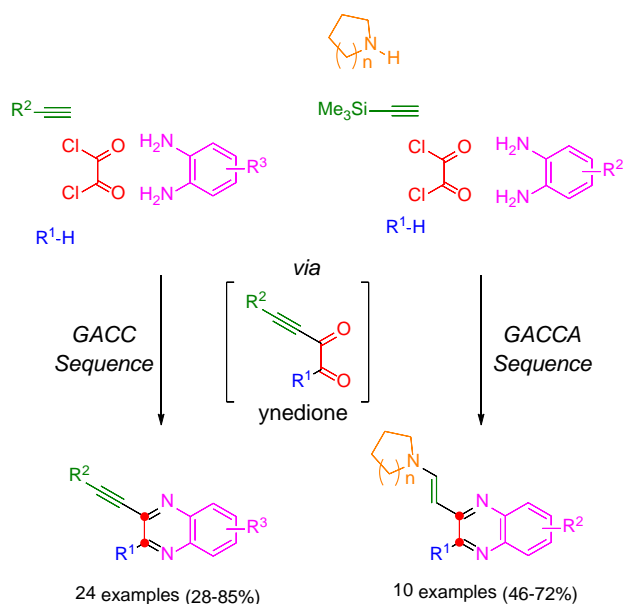


**Figure 1.** Four-component GACC (glyoxylation-alkynylation-cyclocondensation) synthesis of 3-ethynyl quinoxalines and five-component GACCA (glyoxylation-alkynylation-cyclocondensation-addition) synthesis of 3-( $\beta$ -aminovinyl) quinoxalines.

The key intermediate is a densely electrophilic ynedione, which is generated through a copper-catalyzed Stephens-Castro alkylation of the (hetero)aryl glyoxylchloride, formed in a one-pot fashion by glyoxylation of a sufficiently reactive  $\pi$ -nucleophile  $R^1$ -H with oxalyl chloride.<sup>[31]</sup> Alternatively, the (hetero)aryl glyoxylchloride can be generated directly from the (hetero)aryl glyoxylic acid with oxalyl chloride.<sup>[32]</sup> In contrast to Pd-catalyzed alkylation, which proceed with concomitant decarbonylation,<sup>[33]</sup> the Cu-catalyzed variant furnishes the ynedione. The formation of the common 3-ethynyl quinoxaline products or intermediates proceeds via Hinsberg cyclocondensation<sup>[34]</sup> of the ynedione intermediate with *ortho*-phenylene diamine derivatives.<sup>[35]</sup>

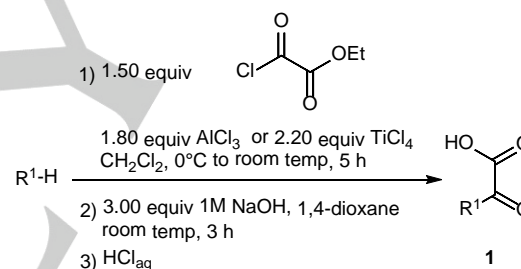
While electron rich  $\pi$ -nucleophiles, in general, are readily employed as substrates in GACC and GACCA sequences, the direct transformation of electroneutral and *para*-substituted benzoid substrates is considerably hampered or impossible. Without any doubt the activation-alkynylation-cyclocondensation (AACC) sequence via the en route generation of (hetero)aryl glyoxylchloride from (hetero)aryl glyoxylic acids and oxalyl chloride<sup>[35]</sup> offers a viable alternative to access ynediones, which already has been employed in a few cases.<sup>[24,29]</sup>

Herein, we report the improved activation-alkynylation-cyclocondensation (AACC) sequence for synthesizing an expanded series of 2-(hetero)aryl substituted 3-ethynyl quinoxalines in the sense of a consecutive three-component synthesis. In addition the photophysical properties are systematically studied by absorption and emission spectroscopy as well as by correlation studies and quantumchemical calculations.

## Results and Discussion

### Synthesis and Structure

Ynediones are densely functionalized polyelectrophilic functional groups with a powerful synthetic potential, which, however, only has scarcely been explored so far.<sup>[36,37]</sup> As already mentioned electron rich  $\pi$ -nucleophiles can be successfully employed in the GACC sequence, however electron rich *para*-substituted arenes, carbazole and benzo[*b*]thiophene derivatives as well as bromo substituted thiophenes could not successfully be transformed (see Supp Inf Tables S1-2). This shortcoming prompted us to directly start from (hetero)aryl glyoxylic acids as starting materials. This alternative route to (hetero)aryl glyoxylchlorides represents an activation, which can be uneventfully performed in a one-pot fashion as well. Therefore, under Friedel-Crafts conditions electron rich *para*-substituted arenes, carbazole and benzo[*b*]thiophene derivatives were reacted with a slight excess of ethoxy oxalyl chloride in the presence of the Lewis acids, such as aluminium chloride or titanium chloride, to give the ethyl (hetero)aryl glyoxylates. The esters were saponified under alkaline conditions giving the desired (hetero)aryl glyoxylic acids **1** in an unpretentious fashion (Scheme 1).<sup>[38-41]</sup> Only very few aryl glyoxylic acids are commercially available.

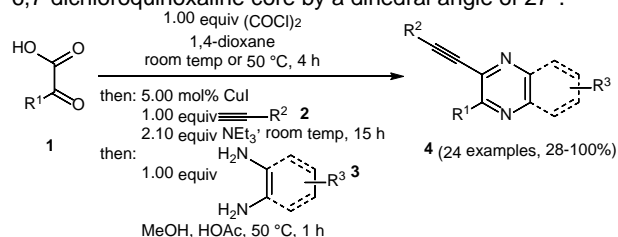


**Scheme 1.** Synthesis of (hetero)aryl glyoxylic acids **1**.

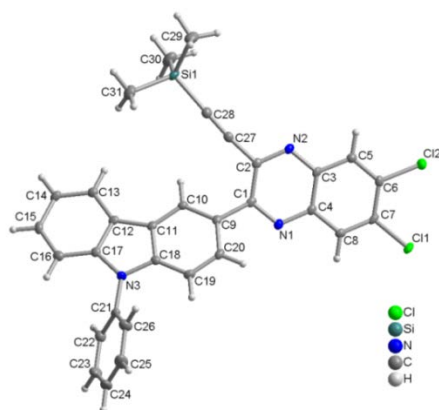
With (hetero)aryl glyoxylic acids **1** in hand the consecutive three-component activation-alkynylation-cyclocondensation (AACC) synthesis of 3-ethynyl quinoxalines **4** commences with the activation of the (hetero)aryl glyoxylic acids **1** with one equivalent of oxalyl chloride at room temp or 50 °C in 1,4-dioxane. The (hetero)aryl glyoxylic chlorides, without isolation, were coupled at room temp with the terminal alkynes **2** in the presence of a catalytic amount of copper(I) iodide and an equimolar amount of triethylamine to form the ynediones. Without isolation, the ynediones are directly reacted with the 1,2-diamino derivatives **3** in the presence of acidic acid and methanol to furnish **24** examples of 2-(hetero)aryl substituted 3-ethynyl quinoxalines **4** in moderate to very good yields (Scheme 2, Table 1).

The proposed structures of the 2-(hetero)aryl substituted 3-ethynyl quinoxalines **4** were unambiguously supported with <sup>1</sup>H and <sup>13</sup>C NMR spectroscopy, mass spectrometry, IR spectroscopy, and combustion analysis. Additionally, the structure of compound **4u** was corroborated by an X-ray crystal structure analysis (Figure 2).<sup>[42]</sup> Compound **4u** crystallizes as

yellow needles in the monoclinic space group  $P2_1/n$ . The 9-phenyl-9*H*-carbazole moiety is twisted out of coplanarity with the 6,7-dichloroquinoxaline core by a dihedral angle of  $27^\circ$ .

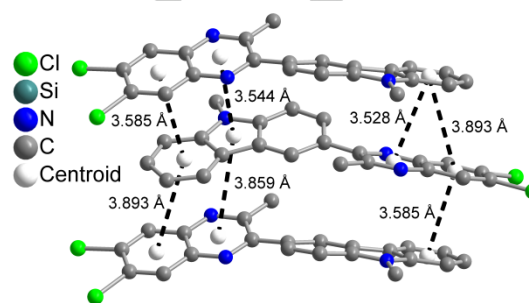


**Scheme 2.** Consecutive three-component activation-alkynylation-cyclocondensation (AACC) synthesis of 2-(hetero)aryl substituted 3-ethynyl quinoxalines **4**.



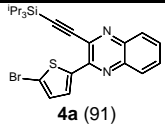
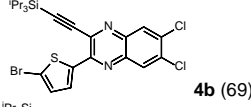
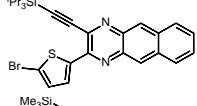
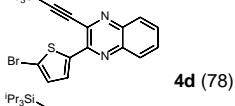
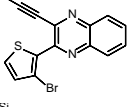
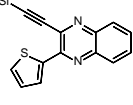
**Figure 2.** Molecular structure of compound **4u** (thermal ellipsoids shown at 50 % probability).

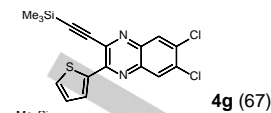
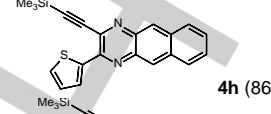
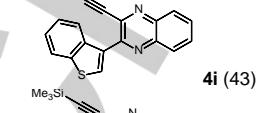
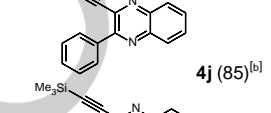
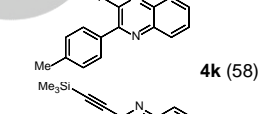
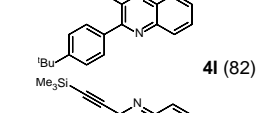
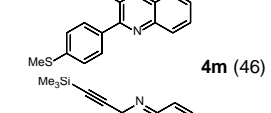
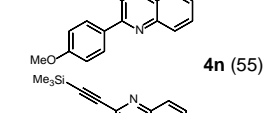
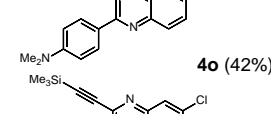
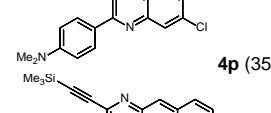
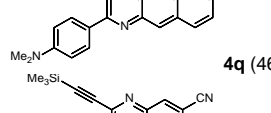
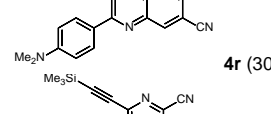
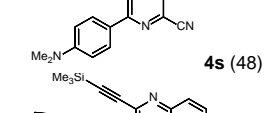
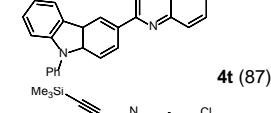
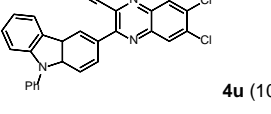
Significant  $\pi$ -stacking shows rather short centroid-centroid contacts ( $< 3.8 \text{ \AA}$ ), near parallel ring planes ( $\alpha < 10^\circ$  to  $\sim 0^\circ$  or even exactly  $0^\circ$  by symmetry), small slip angles ( $\beta, \gamma < 25^\circ$ ) and vertical displacements (slippage  $< 1.5 \text{ \AA}$ ), which translate into a sizable overlap of the aryl-plane areas. (Figure 3).<sup>[43,44]</sup> The molecules are stacked directly on top of each other with sizeable  $\pi$ - $\pi$ -stacking along the *b*-direction and they are arranged in undulated layers parallel to the *ac*-plane.



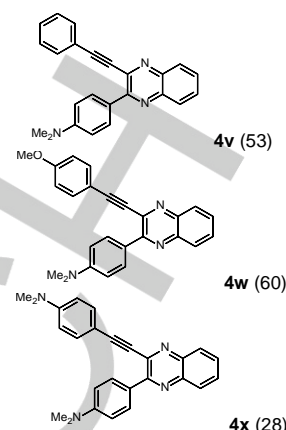
**Figure 3.** Section of the packing diagram of **4u** which shows significant  $\pi$ -stacking interactions along the *b*-direction (labelled with their centroid-centroid distances; from the trimethylsilylethynyl and phenyl groups only the ring-bonded atom have been retained for clarity) (for further details, see Table S6 with additional figures in the Supp Inf).

**Table 1.** Consecutive three-component synthesis of 2-(hetero)aryl substituted 3-ethynyl quinoxalines **4**.

Entry	Glyoxylic acid <b>1</b>	Alkyne <b>2</b>	1,2-Diamino derivative <b>3</b>	2-(Hetero)aryl substituted 3-ethynyl quinoxaline <b>4</b> (yield, %) <sup>[a]</sup>
1	2-bromo-thiophene glyoxylic acid ( <b>1a</b> )	triisopropylsilylacetylene ( <b>2a</b> )	<i>o</i> -phenylene-diamine ( <b>3a</b> )	 <b>4a</b> (91)
2	<b>1a</b>	<b>2a</b>	4,5-dichloro- <i>o</i> -phenylene-diamine ( <b>3b</b> )	 <b>4b</b> (69)
3	<b>1a</b>	<b>2a</b>	2,3-diamino-naphthalene ( <b>3c</b> )	 <b>4c</b> (74)
4	<b>1a</b>	trimethylsilylacetylene ( <b>2b</b> )	<b>3a</b>	 <b>4d</b> (78)
5	3-bromo-thiophene glyoxylic acid ( <b>1b</b> )	<b>2a</b>	<b>3a</b>	 <b>4e</b> (31)
6	2-thiophene glyoxylic acid ( <b>1c</b> )	<b>2b</b>	<b>3a</b>	 <b>4f</b> (88)

7	<b>1c</b>	<b>2b</b>	<b>3b</b>		<b>4g (67)</b>
8	<b>1c</b>	<b>2b</b>	<b>3c</b>		<b>4h (86)</b>
9	benzo[ <i>b</i> ]thiopheneglyoxylic acid ( <b>1d</b> )	<b>2b</b>	<b>3a</b>		<b>4i (43)</b>
10	phenyl glyoxylic acid ( <b>1e</b> )	<b>2b</b>	<b>3a</b>		<b>4j (85)<sup>[b]</sup></b>
11	4-methyl-phenyl-glyoxylic acid ( <b>1f</b> )	<b>2b</b>	<b>3a</b>		<b>4k (58)</b>
12	4- <i>tert</i> -butylphenyl-glyoxylic acid ( <b>1g</b> )	<b>2b</b>	<b>3a</b>		<b>4l (82)</b>
13	4-(methylthio)phenyl-glyoxylic acid ( <b>1h</b> )	<b>2b</b>	<b>3a</b>		<b>4m (46)</b>
14	4-methoxy-phenyl-glyoxylic acid ( <b>1i</b> )	<b>2b</b>	<b>3a</b>		<b>4n (55)</b>
15	4-(dimethyl-amino)-phenyl-glyoxylic acid ( <b>1j</b> )	<b>2b</b>	<b>3a</b>		<b>4o (42%)</b>
16	<b>1j</b>	<b>2b</b>	<b>3b</b>		<b>4p (35)</b>
17	<b>1j</b>	<b>2b</b>	<b>3c</b>		<b>4q (46)</b>
18	<b>1j</b>	<b>2b</b>	4,5-diamino-phthalonitrile ( <b>3d</b> )		<b>4r (30)</b>
19	<b>1j</b>	<b>2b</b>	diamino-maleonitrile ( <b>3e</b> )		<b>4s (48)</b>
20	4-(9 <i>H</i> -carbazol-9-yl)phenyl-glyoxylic acid ( <b>1k</b> )	<b>2b</b>	<b>3a</b>		<b>4t (87)</b>
21	<b>1k</b>	<b>2b</b>	<b>3b</b>		<b>4u (100)</b>

22	1j	phenylacetylene (2c)	3a
23	1j	4-methoxy-phenylacetylene (2d)	3a
24	1j	4-dimethylamino-phenylacetylene (2e)	3a



[a] Yields after chromatography on silica gel. [b] Synthesized according to ref.<sup>[28]</sup>

The presented one-pot protocol for the synthesis of 2-(hetero)aryl substituted 3-ethynyl quinoxalines **4** is particularly interesting since all three reactants **1**, **2**, and **3** are employed in strictly equimolar amounts. In addition upon starting from (hetero)aryl glyoxylic acids **1** the substituent scope in the title compounds at position 2 of the quinoxaline core can be considerably expanded, thereby accessing besides benzoid strong and weak donors as well as electroneutral substitution (Table 1, entries 10-19, 22-24) and heterocyclic derivatives (Table 1, entries 1-9, 20 and 21), all of them are moieties whose (hetero)aromatic precursors are not transformed in the GACC sequence. The diversity pattern of the alkynes is similar as in the GACC sequence, however for the concluding Hinsberg cyclization a slightly broader substitution pattern can be achieved, where not only *o*-phenylenediamine (**3a**), 4,5-dichloro-*o*-phenylenediamine (**3b**), and 2,3-diamino-naphthalene (**3c**) are accepted as substrates, but also the less reactive 1,2-amino derivatives 4,5-diaminophthalonitrile (**3d**) and diaminomaleonitrile (**3e**) are successfully employed at slightly longer reaction times in the terminal step. Thereby, the diacceptor enhanced quinoxaline **4r** (Table 1, entry 18) can be accessed as well as the pyrazine analogue **4s** (Table 1, entry 19).

### Photophysical properties

In previous studies on donor-substituted quinoxalines significantly redshifted emission maxima and large Stokes shifts have been reported.<sup>[24,25,45]</sup> With the library of 2-(hetero)aryl substituted 3-ethynyl quinoxalines **4** in hand systematic investigations of the distinct substituent effects on the optical properties were carried out with quantitative absorption and emission spectroscopy (Table 2). The relative fluorescence quantum yields  $\Phi_F$  were determined with suitable standards according to literature procedures.<sup>[46]</sup>

In the UV/vis absorption spectra, two to four distinct broad structureless maxima can be found and the longest wavelength bands  $\lambda_{max,abs}$  appear between 352 and 484 nm with molar absorption coefficients  $\epsilon$  ranging from 8100 to 29800 L mol<sup>-1</sup> cm<sup>-1</sup>. The remote R<sup>2</sup> substituent at the *para*-position of the arylethynyl moiety only has a minor effect on the energy of this absorption and varies between 421 nm for *N,N*-dimethyl aniline (Table 2, entry 24) to 417 nm for phenyl (Table 2, entry 22).

**Table 2.** Selected photophysical properties of 2-(hetero)aryl substituted 3-ethynyl quinoxalines **4** (recorded in CH<sub>2</sub>Cl<sub>2</sub> at T = 293 K).

Entry	Compound	$\lambda_{max,abs}$ [nm] <sup>[a]</sup> ( $\epsilon$ [L mol <sup>-1</sup> cm <sup>-1</sup> ])	$\lambda_{max,em}$ [nm] <sup>[b]</sup> ( $\Phi_F$ [a.u.])	Stokes shift $\Delta\tilde{\nu}$ [cm <sup>-1</sup> ] <sup>[c]</sup>
1	<b>4a</b>	269.0 (21700), 309.0 (28500), 383.0 (12600)	458.0 (0.19) <sup>[d]</sup>	4300
2	<b>4b</b>	271.5 (34500), 313.0 (12400), 394.5 (15900), 406.0 (15400)	463.0 (0.89) <sup>[e]</sup>	3000
3	<b>4c</b>	300.0 (46000), 344.0 (39800), 409.0 (13000)	519.0 (0.76) <sup>[e]</sup>	5200
4	<b>4d</b>	265.0 (22600), 309.0 (31300), 384.0 (12700)	448.0 (0.16) <sup>[d]</sup>	3700
5	<b>4e</b>	267.0 (39400), 355.0 (10400)	423.0 (0.04) <sup>[d]</sup>	4500
6	<b>4f</b>	265.0 (33000), 377.5 (10900)	430.0 (<0.01) <sup>[d]</sup>	3200
7	<b>4g</b>	270.0 (34800), 293.0 (21800sh), 376.0 (11790), 392.0 (13400)	456.0 (<0.01) <sup>[d]</sup>	4700
8	<b>4h</b>	256.0 (27600sh), 296.5 (40000), 337.5 (30600), 413.0 (9414)	522.0 (0.49) <sup>[e]</sup>	3600
9	<b>4i</b>	264.0 (46800), 303.0 (13700), 371.0 (8100)	458.0 (0.01) <sup>[d]</sup>	5100
10	<b>4j</b>	262.5 (45600), 352.0 (10500)	403.0 (<0.01) <sup>[d]</sup>	3600

11	<b>4k</b>	262.0 (48300), 357.0 (10300)	407.0 (<0.01) <sup>[d]</sup>	3500
12	<b>4l</b>	262.0 (12000), 357.0 (11300)	411.0 (<0.01) <sup>[d]</sup>	3700
13	<b>4m</b>	264.0 (22900), 298.5 (48600), 371.5 (12500)	479.0 (0.07) <sup>[d]</sup>	6000
14	<b>4n</b>	262.0 (54800), 284.0 (24300sh), 368.0 (12100)	444.0 (0.50) <sup>[d]</sup>	4700
15	<b>4o</b>	263.0 (35300), 320.0 (24500), 346.0 (16700sh), 414.0 (9000)	598.0 (0.08) <sup>[f]</sup>	7400
16	<b>4p</b>	250.0 (34500), 333.0 (24000), 360.0 (16700sh), 442.0 (9100)	640.0 (0.07) <sup>[f]</sup>	7000
17	<b>4q</b>	298.0 (39400), 328.0 (25600sh), 424.5 (11000), 470.0 (8100)	659.0 (0.03) <sup>[f]</sup>	8400
18	<b>4r</b>	269.0 (32300), 344.5 (10800), 404.0 (15300), 484.0 (9400)	- <sup>[g]</sup>	-
19	<b>4s</b>	279.0 (20500), 305.0 (20300sh), 452.5 (29800)	- <sup>[g]</sup>	-
20	<b>4t</b>	263.0 (56300), 295.0 (39200), 390.0 (11400)	509.0 (0.38) <sup>[e]</sup>	5100
21	<b>4u</b>	268.0 (43400), 296.0 (29200), 408.0 (11000)	535.0 (0.43) <sup>[e]</sup>	5800
22	<b>4v</b>	265.0 (23500), 279.0 (48700sh), 333.0 (49300), 417.0 (16900)	596.0 (0.23) <sup>[f]</sup>	7200
23	<b>4w</b>	267.0 (44600sh), 310.0 (47900sh), 414.0 (18700)	586.0 (0.42) <sup>[d]</sup>	7100
24	<b>4x</b>	299.0 (58500), 329.0 (57900), 421.0 (22300)	574.0 (0.37) <sup>[f]</sup>	6400

[a] Recorded in CH<sub>2</sub>Cl<sub>2</sub>,  $\alpha(4) = 10^{-5}$  M at  $T = 293$  K. [b] Recorded in CH<sub>2</sub>Cl<sub>2</sub> at room temp, relative quantum yields were determined employing literature procedures ( $\pm 10\%$ ).<sup>[46]</sup> [c]  $\Delta\tilde{\nu} = 1/\lambda_{\max,abs} - 1/\lambda_{\max,em}$ . [d] Recorded at  $\lambda_{ex} = 350$  nm,  $\alpha(4) = 10^{-7}$  M, determined with 9,10-diphenylanthracene (DPA) as a standard in cyclohexane ( $\Phi_F = 1.00$ ). [e] Recorded at  $\lambda_{ex} = 420$  nm,  $\alpha(4) = 10^{-7}$  M, determined with coumarin 153 as a standard in MeOH ( $\Phi_F = 0.45$ ). [f] Recorded at  $\lambda_{ex} = 430$  nm,  $\alpha(4) = 10^{-7}$  M, determined with 4-(dicyanomethylene)-2-methyl-6-(*p*-dimethylaminostyryl)-4*H*-pyran (DCM) in MeOH ( $\Phi_F = 0.43$ ). [g] No signal in CH<sub>2</sub>Cl<sub>2</sub> has been detected.

In the spectra of the consanguineous series of the 2-(*p*-N,N-dimethylanilino)-3-(trimethylsilylethynyl)-substituted quinoxalines **4o-r** it can be clearly seen that the red shift of the longest wavelength absorption band directly correlates with the increasing electron withdrawing power of the quinoxaline moiety in order depicted in Figure 4. This effect expectedly relies on the acceptor character of the substituents and the extension of the  $\pi$ -electron delocalization, as shown by the benzoannellation for compound **4q** in comparison to the mother system **4o**. It is noteworthy to mention that the same qualitative trend is found in the other consanguineous triads **4a-c** and **4f-h** (Table 2, entries 1-3 and 6-8).

All compounds **4** are intensively luminescent in dichloromethane solutions with relative high quantum yields up to 0.89 with Stokes shifts in a range from 3200 to 8400 cm<sup>-1</sup>. Generally, the

Stokes shifts are significantly larger for the *p*-dimethylamino substituent, the strongest donor in the series of compounds **4**, than for other substituents. In the consanguineous series of the compounds **4j-o** (Figure 5) the Stokes shifts' increase obviously correlates with the donor capacities (see also Figure 4). Interestingly, upon enhancing the push-pull nature going to the extremes of strong donors and strong acceptors, as for the chromophores **4r** and **4s**, the emission in dichloromethane vanishes completely. According to the energy gap law,<sup>[47]</sup> where the nonradiative decay of the excited state directly correlates with the redshift of the emission bands, this observation can be additionally supported by the occurrence of fluorescence of these compounds in less polar solvents (*n*-pentane, cyclohexane, toluene).

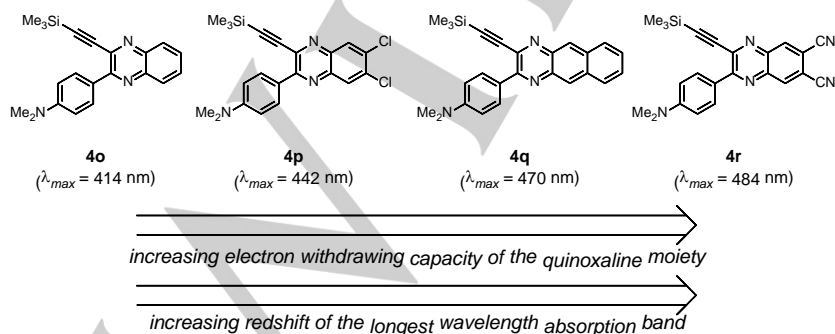


**Figure 4.** Qualitative effect of the electron withdrawing capacity of the quinoxaline core on the absorption properties in the series of 2-(*p*-N,N-dimethylanilino)-3-(trimethylsilylethynyl)-substituted quinoxalines **4o-r**.

For scrutinizing subtle polar electronic substituent effects in the electronic ground and excited state the longest wavelength absorption bands  $\lambda_{max,abs}$ , emission bands  $\lambda_{max,em}$ , and the Stokes shifts  $\Delta\tilde{\nu}$  of the consanguineous series of compounds **4j-o** were correlated with Hammett parameters<sup>[48]</sup>  $\sigma_p$ ,  $\sigma_i$ ,  $\sigma_R$ ,  $\sigma_{p+}$ , and  $\sigma_p$  to establish linear structure-property relationships. In this series the best correlations were found for the correlations with the parameter  $\sigma_{p+}$ , which accounts for substantial involvement of the stabilization of positive charge upon excitation from the ground state ( $\lambda_{max,abs} = 2508.7 \cdot \sigma_{p+} + 28643$  [cm<sup>-1</sup>];  $r^2 = 0.9635$ ), emission from a polar vibrationally relaxed excited singlet state ( $\lambda_{max,em} = 4979.2 \cdot \sigma_{p+} + 25329$  [cm<sup>-1</sup>];  $r^2 = 0.9135$ ), and a pronounced degree of positive emission solvatochromicity as reflected by the negative slope of the Stokes shifts' correlation ( $\Delta\tilde{\nu} = -2470.6 \cdot \sigma_{p+} + 3313.7$  [cm<sup>-1</sup>];  $r^2 = 0.8238$ ) (for details on the failed correlations see Figures S1-5 in Supp Inf). The considerably larger slope of the emission correlation compared to the absorption correlation particularly underlines the very polar nature of the vibrationally relaxed excited state, stemming from a significant charge transfer character of the S<sub>1</sub> state. Since obviously the  $\sigma$  parameters of the methylthio substituent (compound **4m**) overestimate stabilizations of discrete positive charges, resonance contributions and combinations of inductive and resonance effects the correlations of  $\lambda_{max,abs}$ ,  $\lambda_{max,em}$ , and  $\Delta\tilde{\nu}$  with  $\sigma_p$ ,  $\sigma_R$ , and  $\sigma_{p+}$  of the consanguineous series of compounds **4j-o** without compound **4m** give excellent correlations for  $\sigma_p$  and  $\sigma_{p+}$  parameters (see Supp Inf for details), it can be concluded that the remote substituent effect is transferred by both inductive and resonance mechanisms involving considerable charge transfer character.

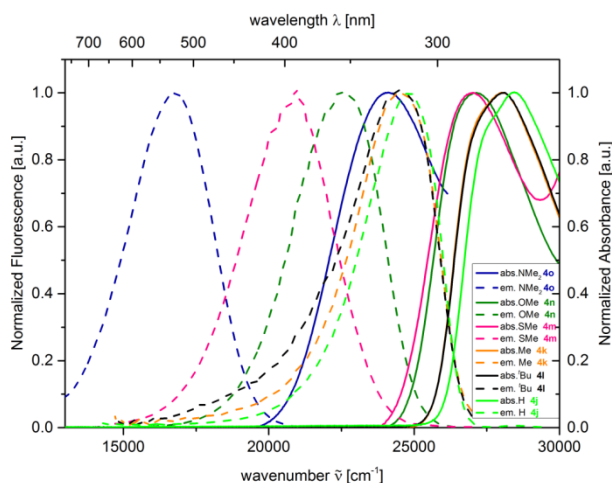


**Figure 5.** Normalized UV/vis absorption (recorded in CH<sub>2</sub>Cl<sub>2</sub>,  $T = 293$  K,  $c(\mathbf{4}) = 10^{-5}$  M, bold line) and emission bands (recorded in CH<sub>2</sub>Cl<sub>2</sub>,  $T = 293$  K,  $c(\mathbf{4}) = 10^{-7}$  M,  $\lambda_{ex} = 430$  nm (**4o**),  $\lambda_{ex} = 350$  nm (**4j-o**, dashed line) of the series **4j-o**.

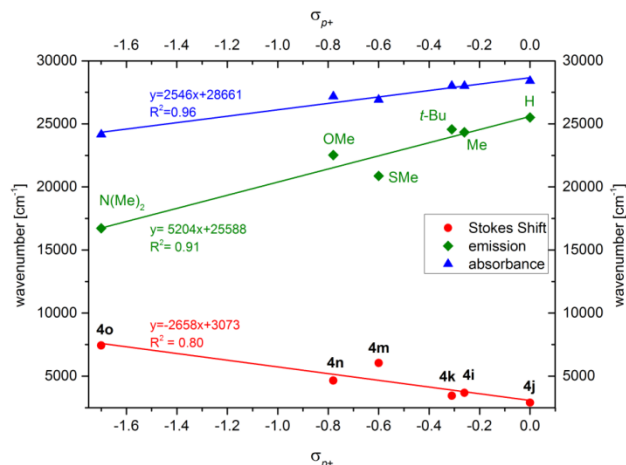


**Figure 6.** Linear correlation plots of the absorption ( $\lambda_{max,abs}$ ), emission maxima ( $\lambda_{max,em}$ ), and Stokes shifts ( $\Delta\tilde{\nu}$ ) [cm<sup>-1</sup>] of 3-ethynyl quinoxalines **4j-o** against the Hammett-parameters  $\sigma_{p+}$ .

The first series of 3-ethynyl quinoxalines with moderately electron releasing indole donors already showed a pronounced emission solvatochromicity.<sup>[29]</sup> Upon enhancing the donor capacity in this second series of 3-ethynyl quinoxalines **4** this effect is even more intense for *N,N*-dimethylaminophenyl derivatives, covering a broad part of the spectral range upon variation of the solvent polarity from *n*-pentane to acetonitrile (Figures 7 and 8). With this respect compound **4p** was quantitatively studied by absorption and emission spectroscopy in solvents of different polarity. The absorption solvatochromicity is only minor and ranges between 430 and 447 nm, while with increasing solvent polarity the emission maximum  $\lambda_{max,em}$  is shifted bathochromically, ranging from greenish-blue luminescence (478 nm) in cyclohexane to red fluorescence in *N,N*-dimethyl formamide (755 nm) (for detailed data see Supp Inf, Table S4). A change in the dipole moment of the fluorophore upon excitation and dipolar relaxation of the surrounding molecules is the origin of the observed emission solvatochromicity.<sup>[49]</sup> This phenomenon is rationalized by several theoretical descriptions, including the Lippert-Mataga model that allows for a quantitative treatment.<sup>[50]</sup>



**Figure 7.** Fluorescence of compound **4p** with variable solvent polarity (from left to right: *n*-pentane, cyclohexane, toluene, 1,4-dioxane, diethylether, ethyl acetate, dichloromethane, *N,N*-dimethyl formamide, acetonitrile;  $\lambda_{ex} = 365$  nm, hand-held UV lamp).

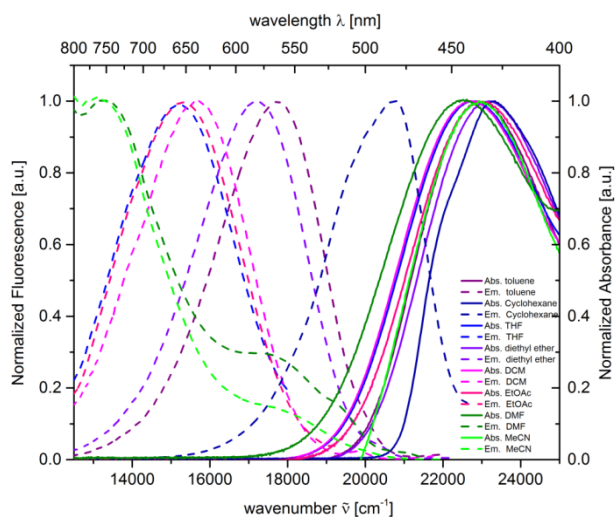


**Figure 8.** UV/vis absorption (solid lines) and emission spectra (dashed lines) of compound **4p**, measured in eight solvents of different polarity (recorded at  $T = 293$  K).

Therefore, for compound **4p** the solvatochromicity was evaluated by determining the Lippert-Mataga orientation polarizability ( $\Delta f$ ) (Equation 1) for an extended set of solvents with variable polarity. Consequently, the Stokes shifts ( $\Delta\tilde{\nu}$ ) were plotted against the  $\Delta f$  values, which can be calculated according to

$$\Delta f = \frac{\epsilon_r - 1}{2\epsilon_r + 1} - \frac{n^2 - 1}{2n^2 + 1} \quad (1)$$

from the relative permittivity  $\epsilon_r$  and the optical refractive index  $n$  of the respective solvent.<sup>[49]</sup>

The Stokes shift  $\Delta\tilde{\nu}$  correlates linearly with the Lippert-Mataga polarity parameters  $\Delta f(\epsilon_r, n)$  with an excellent goodness of fit ( $r^2 = 0.98$ , Figure 9), indicating the dominant importance of a general solvent effect. The change in dipole moment from the electronic ground to the vibrationally relaxed excited state can be calculated according to the Lippert-Mataga equation (Equation 2).

$$\tilde{\nu}_a - \tilde{\nu}_f = \frac{2\Delta f}{hc a^3} (\mu_E - \mu_G)^2 + const \quad (2)$$

While  $\Delta\tilde{\nu}_a$  and  $\Delta\tilde{\nu}_f$  represent the absorption and emission maxima (in  $\text{m}^{-1}$ ),  $\mu_E$  and  $\mu_G$  are the dipole moments in the excited and ground state (in Cm),  $\epsilon_0$  ( $8.8542 \times 10^{-12} \text{ As } V^{-1} \text{ m}^{-1}$ ) is the vacuum permittivity constant,  $h$  ( $6.6256 \times 10^{-34} \text{ J s}$ ) is Planck's constant,  $c$  ( $2.9979 \times 10^8 \text{ ms}^{-1}$ ) is the speed of light, and  $a$  is the radius of the solvent cavity occupied by the molecule (in m).

Assuming a spherical dipole, the Onsager radius  $a$ , which is used to approximate the molecular volume of the molecule in solution, was estimated from the optimized ground-state structure of compound **4p** obtained from DFT calculations (vide infra). Employing a value of  $12.9 \text{ \AA}$  ( $12.9 \times 10^{-10} \text{ m}$ ), the change in dipole moment  $\Delta\mu$  was calculated to  $26 \text{ D}$  ( $8.67 \times 10^{-29} \text{ Cm}$ ). This large value corresponds to a pronounced charge separation upon charge transfer excitation.

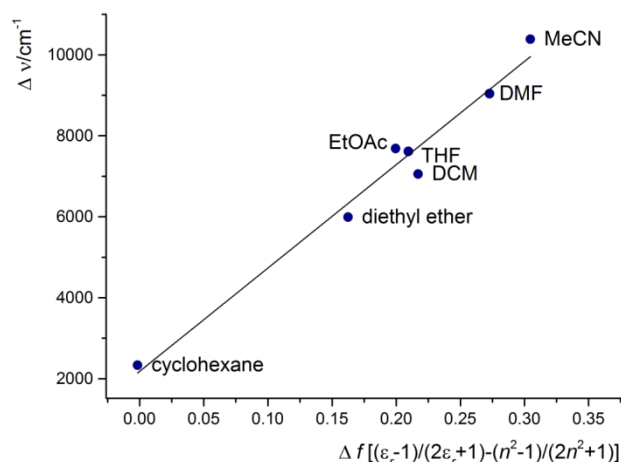


**Figure 9.** Lippert plot for compound **4p** ( $n = 7$ ,  $r^2 = 0.98$ ).

### Calculated electronic structure

A thorough understanding of the photophysical behavior of the consanguineous series of quinoxalines **4o-r** was sought in elucidating the electronic structure by calculating UV/vis absorption spectra at the DFT level of theory, with a special focus on the comparison of the respective quinoxaline core. The geometries of the electronic ground-state structures were optimized by using Gaussian09<sup>[51]</sup> with the PBEH1PBE functional<sup>[52]</sup> and the Pople 6-31G(d) basis set.<sup>[53]</sup> Since absorption properties were measured in dichloromethane solutions, the polarizable continuum model (PCM) with dichloromethane as a solvent was utilized.<sup>[54]</sup> All minimum structures were unambiguously assigned by analytical frequency analysis. The structures were chosen as a series of compounds with four different quinoxaline cores from electron-neutral (**4o** and **4q**) to electron-withdrawing (**4p** and **4r**) properties. The calculated equilibrium ground state structures show that the *p*-dimethylamino substituent adopts angles between  $26$  and  $38^\circ$  (for details on the torsion angles of the computed structures **4o-r** see Supp Inf). Based upon these optimized ground state geometries the electronic transitions  $S_1$  to  $S_4$  were calculated on the TD DFT level of theory (Table 3). The longest wavelength absorption bands are clearly dominated by HOMO-LUMO transitions, which correctly reproduce the experimentally obtained data.

A closer inspection of the coefficient densities in the Kohn-Sham frontier molecular orbitals (FMO) of the four different 3-ethynyl quinoxalines **4o-r** reveals that the HOMO coefficient densities are predominantly localized on the *p*-dimethylamino substituent, while much lower coefficient densities are found on quinoxaline cores (Figure 10). The inverse distribution is observed for the coefficient densities of the LUMOs, which are primarily located on the electron accepting 3-ethynyl quinoxaline cores. Significant FMO orbital coefficients on the quinoxaline moieties are in good agreement with substantial

overlap for the Franck-Condon transitions, resulting in pronounced transition dipole moments and oscillator strengths. In addition the FMO consideration also supports the high degree of charge transfer  $\pi$ - $\pi^*$  character of the longest wavelength absorption bands. Concurrently, this interpretation is in good

agreement with the experimentally observed large solvatochromicity of compound **4p**, supported by the experimentally determined considerable change in dipole moment upon excitation to the vibrationally relaxed  $S_1$  state, which possesses a highly dominant charge transfer character.

**Table 3.** TD-DFT calculations (PBEh1PBE/6-31G(d)) of the UV/vis absorption maxima of the 3-ethynyl quinoxaline **4o-r** applying PCM with dichloromethane as a solvent.

	$\lambda_{max,abs}$ [nm] ( $\epsilon$ [L mol <sup>-1</sup> cm <sup>-1</sup> ]) <sup>[a]</sup>	$\lambda_{max,calcd}$ [nm]	Most dominant contributions	Oscillator strength
<b>4o</b>	414.0 (9000)	424	HOMO→LUMO (98%)	0.103
	346.0 (16700sh)	331	HOMO→LUMO+1 (90%)	0.380
	320.0 (24500)	303	HOMO-1→LUMO (79%) HOMO→LUMO+1 (7%)	0.390
	263.0 (35300)	265	HOMO-1→LUMO+1 (63%) HOMO-6→LUMO+1 (8%) HOMO-3→LUMO+1 (8%)	0.577
<b>4p</b>	442.0 (9100)	457	HOMO→LUMO (98%)	0.140
	360.0 (16700sh)	347	HOMO→LUMO+2 (87%)	0.404
	333.0 (24000)	319	HOMO-1→LUMO (79%) HOMO→LUMO+2 (6%) HOMO-2→LUMO (6%)	0.468
	250.0 (34500sh)	265	HOMO→LUMO+3 (52%) HOMO→LUMO+4 (26%) HOMO→LUMO+6 (12%)	0.087
<b>4q</b>	470.0 (8100)	475	HOMO→LUMO (98%)	0.135
	424.5 (11000)	403	HOMO-1→LUMO (90%) HOMO-3→LUMO (6%)	0.085
	328.0 (25600sh)	322	HOMO→LUMO+1 (58%) HOMO-2→LUMO (20%) HOMO-1→LUMO+1 (18%) HOMO-1→LUMO+1 (32%)	0.669
	298.0 (39400)	285	HOMO→LUMO+2 (26%) HOMO-2→LUMO (16%) HOMO-5→LUMO (11%)	0.789
<b>4r</b>	484.0 (9400)	494	HOMO→LUMO (98%)	0.118
	404.0 (15300)	390	HOMO→LUMO+1 (95%)	0.489
	344.5 (10800)	323	HOMO-1→LUMO (65%) HOMO-2→LUMO (9%)	0.246
	269.0 (32300)	277	HOMO-2→LUMO+1 (63%) HOMO→LUMO+4 (16%)	0.003

[a] Recorded in dichloromethane,  $T = 293$  K,  $c(\mathbf{4o-s}) = 10^{-5}$  M.

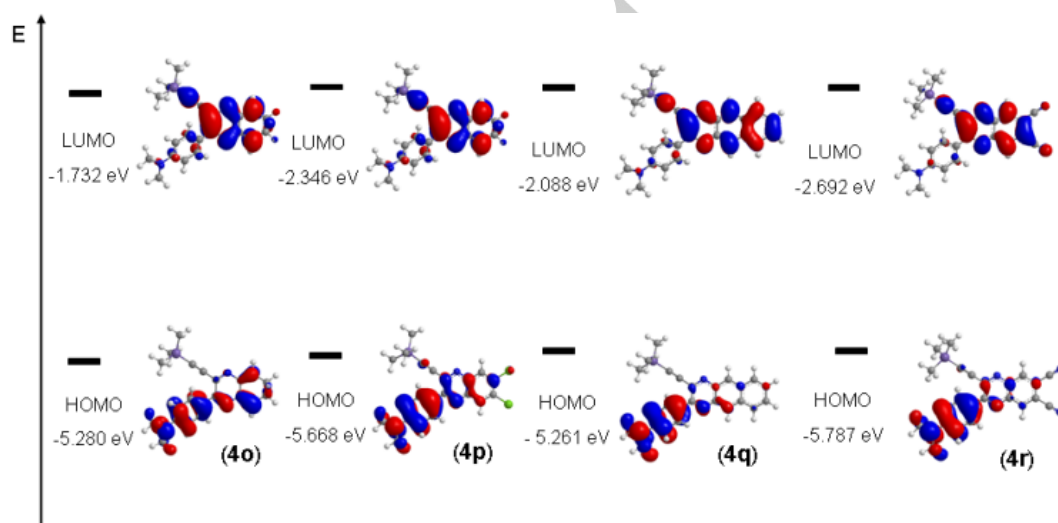


**Figure 10.** Selected DFT-computed (PBEh1PBE/6-31G(d)) Kohn-Sham frontier molecular orbitals for **4o-r**.

## Conclusions

In conclusion we have successfully synthesized a series of diversity-oriented 2-substituted 3-ethynyl quinoxaline chromophores by applying the consecutive three-component activation-alkynylation-cyclocondensation (AACC) protocol. Thereby 2-substituents at the quinoxaline core can be readily introduced, which either very difficult or impossible to introduce by our previous glyoxylation-alkynylation-cyclocondensation (GACC) approach. A series of donor-acceptor conjugates become accessible, in particular, by placing the *p*-dimethylamino substituent as a strong donor. As a result the positive emission solvochromicity is considerably enhanced in comparison to the first generation of 3-ethynyl quinoxalines, causing a shift of the emission color over a broad part of the spectral range by variation of the solvent polarity. The highly polar nature of the excited state is experimentally elucidated by linear structure-property relationships of the Hammett  $\sigma_{p+}$  parameters with the absorption and emission bands and the Stokes shifts, as well as by Lippert-Mataga determination of the change of dipole moment upon photonic excitation. In addition the photophysical behavior is supported by DFT and TD-DFT calculations, employing the PBEh1PBE functional, which better reproduces the charge transfer character of the longest wavelength absorption bands. These emission solvatochromic dyes with enhanced donor capacity are particularly well suited as highly sensitive polarity sensors. Studies to increase the substituent diversity on quinoxaline acceptors by multicomponent strategies and the modulation of the polar excited states by variation of the employed donor and acceptor moieties are currently underway.

Supporting information for this article is available on the WWW under <http://dx.doi.org/10.1002/chem.2014xxxxx>. Study on glyoxylation-alkynylation-cyclocondensation sequences with anilines and other  $\pi$ -nucleophiles, experimental details and full characterization of compounds **4**,  $^1\text{H}$  and  $^{13}\text{C}$  NMR spectra of compounds **4**, absorption and emission spectra of compounds **4**, Hammett correlations, solvatochromism, X-ray and DFT computed XYZ-coordinates and energies of structures **4o-r**.

## Experimental Section

**Typical procedure for the three-component synthesis of 2-(thiophen-2-yl)-3-((trimethylsilyl)ethynyl)quinoxaline (4f).** Glyoxylic acid **1c** (314 mg, 2.00 mmol) was placed in dry 1,4-dioxane (5 mL) under an argon atmosphere in a sintered screw-cap Schlenk tube and the solution was then deaerated degassed with argon (5 min). The mixture was stirred at room temp (water bath) for 5 min. Thereafter, the mixture was stirred at room temp (water bath) for 4 h. Then the mixture was cooled to room temp (water bath) for 5 min. Then, CuI (20 mg, 0.10 mmol, 5.00 mol %), alkyne **2b** (0.28 mL, 2.00 equiv), and dry triethylamine (0.59 mL, 4.20 mmol) were successively added to the reaction mixture, and stirring at room temp was continued for 16 h. Then, methanol (2 mL), 1,2-diaminoarene **3a** (216 mg, 2.00 mmol) and of acetic acid (0.24 mL, 4.00 mmol) were added successively to the reaction mixture. The mixture was

stirred at 50 °C for 1 h, water (10 mL) was added and the aqueous phase was extracted with dichloromethane (3 x 5 mL/10 mL, monitored by TLC). The combined organic layers were dried (anhydrous sodium sulfate) and the solvents were removed in vacuo. The residue was absorbed onto Celite® and purified by flash chromatography on silica gel (petroleum ether (boiling range 40–60 °C)/ethyl acetate) to give 3-ethynylchinoxaline **4f** (540 mg, 88%) as a yellow solid,  $R_f = 0.22$  (petroleum ether/ethyl acetate 25:1). Mp 93 °C.  $^1\text{H}$  NMR ( $\text{CDCl}_3$ , 300 MHz):  $\delta$  0.37 (s, 9 H), 7.18 (dd,  $J = 5.1, 3.9$  Hz, 1 H), 7.57 (dd,  $J = 5.1, 1.1$  Hz, 1 H), 7.66–7.78 (m, 2 H), 7.99–8.09 (m, 2 H), 8.56 (dd,  $J = 3.9, J = 1.1$  Hz, 1 H).  $^{13}\text{C}$  NMR ( $\text{CDCl}_3$ , 75 MHz):  $\delta$  -0.44 ( $\text{CH}_3$ ), 102.8 ( $\text{C}_{\text{quat}}$ ), 103.2 ( $\text{C}_{\text{quat}}$ ), 127.9 (CH), 128.8 (CH), 128.9 (CH), 130.0 (CH), 130.3 (CH), 130.5 (CH), 131.1 (CH), 134.9 ( $\text{C}_{\text{quat}}$ ), 140.4 ( $\text{C}_{\text{quat}}$ ), 140.7 ( $\text{C}_{\text{quat}}$ ), 141.9 ( $\text{C}_{\text{quat}}$ ), 147.7 ( $\text{C}_{\text{quat}}$ ). EI-MS ( $m/z$ ): 309 (15), 308 ( $[\text{M}]^+$ , 58), 307 (33), 295 (10), 294 ( $[\text{M}-\text{CH}_3]^+$ , 24), 295 ( $[\text{M}-\text{CH}_3]^+$ , 100), 277 ( $[\text{M}-\text{CH}_3]_2^+$ , 9), 263 ( $[\text{M}-\text{CH}_3]_3^+$ , 19). IR [ $\text{cm}^{-1}$ ]:  $\tilde{\nu}$  3125 (w), 3102 (w), 3065 (w), 2957 (w), 2922 (w), 2901 (w), 2855 (w), 2164 (w), 1558 (w), 1526 (w), 1472 (w), 1460 (w), 1427 (m), 1393 (w), 1362 (w), 1335 (m), 1315 (w), 1300 (w), 1248 (m), 1231 (m), 1219 (m), 1179 (m), 1134 (m), 1119 (w), 1082 (w), 1059 (w), 947 (w), 912 (w), 843 (s), 810 (m), 799 (w), 760 (s), 739 (m), 708 (s), 662 (m), 631 (m), 617 (m). Anal. calcd. for  $\text{C}_{17}\text{H}_{16}\text{N}_2\text{Si}$  (308.1): C 66.19, H 5.23, N 9.08, S 10.39; Found: C 66.46, H 5.33, N 8.78, S 10.12. 314 mg (2.00 mmol) of **1c**

### Typical procedure for the three-component synthesis of 4-(6,7-dichloro-3-((trimethylsilyl)ethynyl)quinoxalin-2-yl)-*N,N*-dimethylaniline (4p).

Glyoxylic acid **1j** (386 mg, 2.00 mmol) was placed in dry 1,4-dioxane (5 mL) under an argon atmosphere in a sintered screw-cap Schlenk tube and the solution was then deaerated degassed with argon (5 min). The mixture was stirred at room temp (water bath) for 5 min. Thereafter, the mixture was stirred at 50 °C (oil bath) for 4 h. Then the mixture was cooled to room temp (water bath) for 5 min. Then, CuI (20 mg, 0.10 mmol, 5.00 mol %), alkyne **2b** (0.28 mL, 2.00 equiv), and dry triethylamine (0.59 mL for 2.00 mmol, 4.20 mmol, 2.10 equiv) were successively added to the reaction mixture, and stirring at room temp was continued for 16 h. Then, methanol (2 mL), 1,2-diaminoarene **3b** (361 mg, 2.00 mmol) and of acetic acid (0.24 mL, 4.00 mmol) were added successively to the reaction mixture. The mixture was stirred at 50 °C for 1 h, water (10 mL) was added and the aqueous phase was extracted with dichloromethane (3 x 5 mL/10 mL, monitored by TLC). The combined organic layers were dried (anhydrous sodium sulfate) and the solvents were removed in vacuo. The residue was absorbed onto Celite® and purified by flash chromatography on silica gel (petroleum ether (boiling range 40–60 °C)/ethyl acetate) to give 3-ethynylchinoxaline **4p** (241 mg, 35%) as an orange solid,  $R_f = 0.10$  (petroleum ether/ethyl acetate 6:1). Mp 186 °C.  $^1\text{H}$  NMR ( $\text{CDCl}_3$ , 300 MHz):  $\delta$  0.22 (s, 9 H), 3.00 (s, 6 H), 6.68–6.74 (m, 2 H), 8.04–8.11 (m, 4 H).  $^{13}\text{C}$  NMR ( $\text{CDCl}_3$ , 75 MHz):  $\delta$  -0.4 ( $\text{CH}_3$ ), 40.4 ( $\text{CH}_3$ ), 102.9 ( $\text{C}_{\text{quat}}$ ), 103.4 ( $\text{C}_{\text{quat}}$ ), 111.4 (CH), 129.2 ( $\text{C}_{\text{quat}}$ ), 129.6 ( $\text{C}_{\text{quat}}$ ), 131.3 ( $\text{C}_{\text{quat}}$ ), 133.6 (CH), 135.1 (CH), 138.2 (CH), 138.9 (CH), 140.0 (CH), 151.8 (CH), 155.2 (CH). EI-MS ( $m/z$ ): 415 ( $[\text{M}]^{+37}\text{Cl}$ ), 21), 414 (13), 413 ( $[\text{M}]^{+35}\text{Cl}$ ), 28), 322 (14), 141 (13), 129 (18), 111 ( $^{37}\text{Cl}$ ), 14), 109 ( $^{35}\text{Cl}$ ), 5), 97 ( $[\text{M}^{37}\text{Cl}]\text{-Si}(\text{CH}_3)_3^+$ , 17), 95 ( $[\text{M}^{35}\text{Cl}]\text{-Si}(\text{CH}_3)_3^+$ , 7), 85 ( $^{37}\text{Cl}$ ), 26), 83 ( $^{35}\text{Cl}$ ), 15), 71 ( $^{35}\text{Cl}$ ), 31), 69 ( $^{37}\text{Cl}$ ), 17), 57 ( $^{37}\text{Cl}$ ), 47), 55 ( $^{35}\text{Cl}$ ), 22) 43 ( $^{37}\text{Cl}$ ), 36), 41 ( $^{35}\text{Cl}$ ), 17). IR [ $\text{cm}^{-1}$ ]:  $\tilde{\nu}$  3107 (w), 3086 (w), 2955 (w), 2897 (w), 2866 (w), 2824 (w), 2803 (w), 2783 (w), 2745 (w), 2475 (w), 2158 (w), 1603 (m), 1530 (m), 1512 (m), 1479 (w), 1443 (m), 1408 (m), 1393 (m), 1373 (m), 1314 (m), 1246 (m), 1233 (m), 1190 (m), 1165 (s), 1099 (m), 1065 (m), 1020 (w), 976 (m), 949 (m), 866 (m), 839 (s), 820 (s), 791 (m), 760 (s), 739 (m), 704 (m), 687 (m), 664 (m), 650 (m), 629 (m). Anal. calcd. for  $\text{C}_{21}\text{H}_{21}\text{Cl}_2\text{N}_3\text{Si}$  (415.0): C 54.11, H 3.74, N 7.42, S 8.50; Found: C 54.40, H 3.95, N 7.20, S 8.20.

## Acknowledgments

We cordially thank Fonds der Chemischen Industrie and Deutsche Forschungsgemeinschaft (Mu 1088/9-1) for the financial support. Computational support and infrastructure was provided by the "Centre for Information and Media Technology" (ZIM) at the University of Düsseldorf (Germany). The authors cordially thank Tobias Wilcke (Heinrich-Heine-Universität Düsseldorf) for taking the photograph for the graphical abstract.

**Keywords:** Absorption • Copper • Cross-coupling • DFT-calculations • Fluorescence • Heterocycles • Multi-component reactions • Solvatochromism

## References:

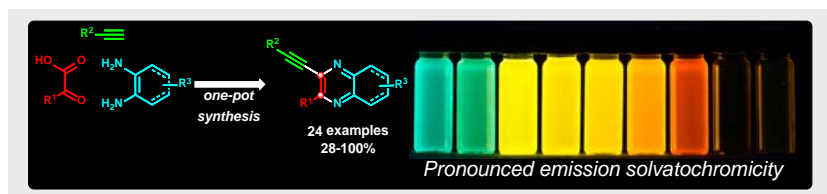
- [1] *Functional Organic Materials*; T. J. J. Müller, U. H. F. Bunz, eds.; Wiley-VCH, Weinheim, **2007**.
- [2] S. R. Forrest, Thompson, M. E. *Chem. Rev.* **2007**, *107*, 923–924.
- [3] For reviews on OFETs, see e. g. a) L. Torsi, M. Magliulo, K. Manoli, G. Palazzo, *Chem. Soc. Rev.* **2013**, *42*, 8612–8628. b) M. Mas-Torrent, C. Rovira, *Chem. Soc. Rev.* **2008**, *37*, 827–838. For reviews on OLEDs, see e. g. c) N. Thejo Kalyania, S. J. Dhoble, *Renew. Sust. Energ. Rev.* **2012**, *16*, 2696–2723. d) K. T. Kamtekar, A. P. Monkman, M. R. Bryce, *Adv. Mater.* **2010**, *22*, 572–582. For a review on DSSCs, see e. g. e) A. Hagfeldt, G. Boschloo, L. Sun, L. Kloo, H. Pettersson, *Chem. Rev.* **2010**, *110*, 6595–6663. f) N. Prabavathy, S. Shalini, R. Balasundaraprabhu, D. Velauthapillai, S. Prasanna, N. Muthukumarasamy, *Int. J. Energy Res.* **2017**, *41*, 1372–1396.
- [4] a) G. S. Loving, M. Sainlos, B. Imperiali, *Trends Biotechnol.* **2010**, *28*, 73–83. (b) Z. Zhang, Y. Zheng, Z. Sun, Z. Dai, Z. Tang, J. Ma, C. Maa, *Adv. Synth. Catal.* **2017**, *359*, 2259–2268.
- [5] a) K. P. Carter, A. M. Young, A. E. Palmer, *Chem. Rev.* **2014**, *114*, 4564–4601. (b) H. Kobayashi, M. Ogawa, R. Alford, P. L. Choyke, Y. Urano, Y. *Chem. Rev.* **2010**, *110*, 2620–2640.
- [6] A. P. Demchenko, Y. Mély, G. Duportail, A. S. Klymchenko, *Biophys. J.* **2009**, *96*, 3461–3470.
- [7] A. Hantzsch, *Ber. Dtsch. Chem. Ges.* **1922**, *55*, 953–979.
- [8] Z. R. Grabowski, K. Rotkiewicz, W. Rettig, *Chem. Rev.* **2003**, *103*, 3899–4031.
- [9] a) M. D. Burke, S. L. Schreiber, *Angew. Chem. Int. Ed.* **2004**, *43*, 46–58. b) E. Ruijter, R. Scheffelaar, R. V. A. Orru, *Angew. Chem. Int. Ed.* **2011**, *50*, 6234–6346.
- [10] T. J. J. Müller, In *Relative Reactivities of Functional Groups as the Key to Multicomponent Reactions in Multicomponent Reactions 1*, T. J. J. Müller, (ed.), Science of Synthesis, Georg Thieme Verlag, Stuttgart, 2014, pp 5–27.
- [11] a) D. M. D'Souza, T. J. J. Müller, *Pure Appl. Chem.* **2008**, *80*, 609–620. b) L. Levi, T. J. J. Müller, *Eur. J. Org. Chem.* **2016**, 2907–2918.
- [12] a) L. Levi, T. J. J. Müller, *Chem. Soc. Rev.* **2016**, *45*, 2825–2846. b) F. de Moliner, N. Kiehlund, R. Lavilla, M. Vendrell, *Angew. Chem. Int. Ed.* **2017**, *56*, 3758–3769. c) R. Riva, L. Moni, T. J. J. Müller, *Targets in Heterocyclic Systems* **2016**, *20*, 85–112. d) T. J. J. Müller in *Aggregation Induced Emission: Materials and Applications*, M. Fujiki, B. Z. Tang, B. Liu, eds., ACS Symposium Series e-book, **2016**, Chapter 6, pp 85–112.
- [13] F. Yu, S.-C. Cui, X. Li, Y. Peng, Y. Yu, K. Yun, S.-C. Zhang, J. Li, J.-G. Liu, J. Hua, *Dyes Pigment.* **2017**, *139*, 7–18.
- [14] K. R. J. Thomas, M. Velusamy, J. T. Lin, C.-H. Chuen, Y.-T. Tao, *Chem. Mater.* **2005**, *17*, 1860–1866.
- [15] L. Liu, G. Zhang, B. He, S. Liu, C. Duan, F. Huang, *Mater. Chem. Front.* **2017**, *1*, 499–506.
- [16] K. Pei, Y. Wu, A. Islam, S. Zhu, L. Han, Z. Geng, W. Zhu, *J. Phys. Chem. C* **2014**, *118*, 16552–16561.
- [17] J. Yuan, L. Qiu, Z. Zhang, Y. Li, Y. He, L. Jiang, Y. Zou, *Chem. Commun.* **2016**, *52*, 6881–6884.
- [18] M. Eugenio Vázquez, J. B. Blanco, B. Imperiali, *J. Am. Chem. Soc.* **2005**, *127*, 1300–1306.
- [19] L. E. Seitz, W. J. Suling, R. C. Reynolds, *J. Med. Chem.* **2002**, *45*, 5604–5606.
- [20] C. Duan, F. Huang, Y. Cao, *J. Mater. Chem.* **2012**, *22*, 10416–10434.
- [21] H. Hayashi, A. S. Touchy, Y. Kinjo, K. Kurotobi, Y. Toude, S. Ito, H. Saarenp, N. V. Tkachenko, H. Lemmetyinen, H. Imahori, *ChemSusChem* **2013**, *6*, 508–517.
- [22] a) Recent review on luminescent quinoxalines, see e. g. S. Achelle, C. Baudequin, N. Plé, *Dyes Pigm.* **2013**, *98*, 575–600. b) S. Achelle, A. Barsella, C. Baudequin, B. Caro, F. Robin-le Guen, *J. Org. Chem.* **2012**, *77*, 4087–4096. c) H. Wang, G. Chen, Y. Liu, I. Hu, X. Xu, S. Ji, *Dyes. Pigm.* **2009**, *83*, 269–275. d) K. J. R. Thomas, J. T. Lin, Y.-T. Tao, C.-H. Chuen, *Chem. Mater.* **2002**, *14*, 2796–2802. e) K. J. R. Thomas, M. Velusamy, J. T. Lin, C.-H. Chuen, Y.-T. Tao, *Chem. Mater.* **2005**, *17*, 1860–1866.
- [23] Y. Wu, W. Zhu, *Chem. Soc. Rev.* **2013**, *42*, 2039–2058.
- [24] C. F. Gers-Panther, H. Fischer, J. Nordmann, T. Seiler, T. Behnke, C. Würth, W. Frank, U. Resch-Genger, T. J. J. Müller, *J. Org. Chem.* **2017**, *82*, 567–578.
- [25] H. T. Black, I. Pelse, R. M. W. Wolfe, J. R. Reynolds, *Chem. Commun.* **2016**, *52*, 12877–12880.
- [26] K. Kudo, A. Momotake, Y. Kanna, Y. Nishimura, T. Arai, *Chem. Commun.* **2011**, *47*, 3867–3869.
- [27] K. Kudo, A. Momotake, J. K. Tanaka, Y. Miwa, T. Arai, *Photochem. Photobiol. Sci.* **2012**, *11*, 674–678.
- [28] a) D. W. Chang, H. J. Lee, J. H. Kim, S. Y. Park, S. M. Park, L. Dai, J. B. Baek, *Org. Lett.* **2011**, *13*, 3880–3883. b) K. Pei, Y. Z. Wu, W. J. Wu, Q. Zhang, B. Q. Chen, H. Tian, W. H. Zhu, *Chem. J. Eur.* **2012**, *18*, 8190–8200.

- [29] C. F. Gers, J. Nordmann, C. Kumru, W. Frank, T. J. J. Müller, *J. Org. Chem.* **2014**, *79*, 3296–3310.
- [30] Z. Zhang, Z. Dai, X. Jiang, *Asian J. Org. Chem.* **2015**, *4*, 1370–1374.
- [31] E. Merkul, J. Dohe, C. Gers, F. Rominger, T. J. J. Müller, *Angew. Chem. Int. Ed.* **2011**, *50*, 2966–2969.
- [32] C. Boersch, E. Merkul, T. J. J. Müller, *Angew. Chem. Int. Ed.* **2011**, *50*, 10448–10452.
- [33] E. Merkul, T. Oeser, T. J. J. Müller, *Chem. Eur. J.* **2009**, *15*, 5006–5011.
- [34] a) O. Hinsberg, *Ber. Dtsch. Chem. Ges.* **1884**, *17*, 318–323. b) G. Körner, *Ber. Dtsch. Chem. Ges.* **1884**, *17*, A572–A573.
- [35] a) S. Gobec, U. Urleb, *Quinoxalines in Science of Synthesis* **2003**, *16*, 848–852. b) D. F. Saifina, N. A. Mamedov, *Russ. Chem. Rev.* **2010**, *79*, 351–370.
- [36] M. Guo, D. Li, Z. Zhang, *J. Org. Chem.* **2003**, *68*, 10172–10174.
- [37] Z. Zhang, X. Jiang, *Org. Lett.* **2014**, *16*, 4400–4403.
- [38] A. Ianni, S. R. Waldvogel, *Synthesis* **2006**, *13*, 2103–2112.
- [39] B. Unterhalt, P. Gores, *Arch. Pharm.* **1989**, *322*, 839–840.
- [40] A. R. Katritzky, B. Galuszka, S. Rachwalsand, D. Lynch, *Org. Prep. Proc. Int.*, **1993**, *25*, 557–562.
- [41] I. T. Barnish, P. E. Cross, J. C. Danilewicz, R. P. Dickinson, D. A. Stopher, *J. Med. Chem.* **1981**, *24*, 399–404.
- [42] Crystallographic data (excluding structure factors) for the structure reported in this paper have been deposited with the Cambridge Crystallographic Data Centre as supplementary publication no. CCDC 1813052 (**4u**). See Table S5 in Supp Inf for a summary of the X-ray structure data.
- [43] a) X.-J. Yang, F. Drepper, B. Wu, W.-H. Sun, W. Haehnel, C. Janiak, *Dalton Trans.* **2005**, 256–267. b) C. Janiak, *J. Chem. Soc. Dalton Trans.* **2000**, 3885–3896.
- [44] a) V. Lozan, P.-G. Lassahn, C. Zhang, B. Wu, C. Janiak, G. Rheinwald, H. Lang, *Z. Naturforsch. B* **2003**, *58*, 1152–1164. b) C. G. Zhang, C. Janiak, *Anorg. Allg. Chem.* **2001**, *627*, 1972–1975. c) C. G. Zhang, C. Janiak, *J. Chem. Crystallogr.* **2001**, *31*, 29–35. d) H.-P. Wu, C. Janiak, G. Rheinwald, H. Lang, *J. Chem. Soc. Dalton Trans.* **1999**, 183–190. e) C. Janiak, L. Uehlin, H.-P. Wu, P. Klüfers, H. Piotrowski, T. G. Scharmann, *J. Chem. Soc., Dalton Trans.* **1999**, 3121–3131. f) H.-P. Wu, C. Janiak, L. Uehlin, P. Klüfers, P. Mayer, *Chem. Commun.* **1998**, 2637–2638.
- [45] A. Ekbote, T. Jadhav, R. Misra, *New J. Chem.* **2017**, *41*, 9346–9353.
- [46] S. Fery-Forgues, D. Lavabre, *J. Chem. Educ.* **1999**, *76*, 1260–1264.
- [47] J. R. Lakowicz, *Principles of Fluorescence Spectroscopy*, 3rd ed.; Springer: Berlin/Heidelberg, **2006**; pp 687–688.
- [48] C. Hansch, A. Leo, R. W. Taft, *Chem. Rev.*, **1991**, *91*, 165–195.
- [49] J. R. Lakowicz, *Principles of Fluorescence Spectroscopy*, 3rd ed.; Springer: Berlin/Heidelberg, **2006**; pp 213–216.
- [50] a) Z. E. Lippert, *Elektrochem.* **1957**, *61*, 962–975. b) N. Mataga, Y. Kaifu, M. Koizumi, *Bull. Chem. Soc. Jpn.*, **1956**, *29*, 465–470.
- [51] M. J. Frisch, G. W. Trucks, H. B. Schlegel, G. E. Scuseria, M. A. Robb, J. R. Cheeseman, G. Scalmani, V. Barone, B. Mennucci, G. A. Petersson, H. Nakatsuji, M. Caricato, X. Li, H. P. Hratchian, A. F. Izmaylov, J. Bloino, G. Zheng, J. L. Sonnenberg, M. Hada, M. Ehara, K. Toyota, R. Fukuda, J. Hasegawa, M. Ishida, T. Nakajima, Y. Honda, O. Kitao, H. Nakai, T. Vreven, J. A. Montgomery, Jr., J. E. Peralta, F. Ogliaro, M. Bearpark, J. J. Heyd, E. Brothers, K. N. Kudin, V. N. Staroverov, R. Kobayashi, J. Normand, K. Raghavachari, A. Rendell, J. C. Burant, S. S. Iyengar, J. Tomasi, M. Cossi, N. Rega, J. M. Millam, M. Klene, J. E. Knox, J. B. Cross, V. Bakken, C. Adamo, J. Jaramillo, R. Gomperts, R. E. Stratmann, O. Yazyev, A. J. Austin, R. Cammi, C. Pomelli, J. W. Ochterski, R. L. Martin, K. Morokuma, V. G. Zakrzewski, G. A. Voth, P. Salvador, J. J. Dannenberg, S. Dapprich, A. D. Daniels, O. Farkas, J. B. Foresman, J. V. Ortiz, J. Cioslowski, D. J. Fox, *GAUSSIAN 09 (Revision A.02)* Gaussian, Inc., Wallingford CT, **2009**.
- [52] a) C. Lee, W. Yang, R. G. Parr, *Phys. Rev. B: Condens. Matter Mater. Phys.* **1988**, *37*, 785–789. b) A. D. Becke, *J. Chem. Phys.* **1993**, *98*, 1372–1377. c) K. Kim, K. D. Jordan, *J. Phys. Chem.* **1994**, *98*, 10089–10094. d) P. J. Stephens, F. J. Devlin, C. F. Chabalowski, M. J. Frisch, *J. Phys. Chem.* **1994**, *98*, 11623–11627.
- [53] R. Krishnan, J. S. Binkley, R. Seeger, J. A. Pople, *J. Chem. Phys.* **1980**, *72*, 650–654.
- [54] G. Scalmani, M. J. Frisch, *J. Chem. Phys.* **2010**, *132*, 114110.

## Entry for the Table of Contents

Layout 2:

## FULL PAPER



Franziska K. Merkt,<sup>a</sup> Simon P. Höwedes,<sup>a</sup> Charlotte F. Gers-Panther,<sup>a</sup> Irina Gruber,<sup>b</sup> Christoph Janiak,<sup>b</sup> and Thomas J. J. Müller<sup>\*a</sup>

Page No. – Page No.

**Three-component Activation-  
Alkynylation-Cyclocondensation  
(AACC) Synthesis of Enhanced  
Emission Solvatochromic 3-Ethynyl  
Quinoxalines**

A consecutive activation-alkynylation-cyclocondensation sequence efficiently furnishes 2-substituted 3-ethynyl quinoxaline chromophores in a consecutive three-component fashion. *N,N*-Dimethyl aniline in position 2 causes a considerable enhanced emission solvatochromicity, rationalized by TD-DFT calculations, Hammett correlations and Lippert-Mataga analysis, with a spectral range from blue green to deep red orange with a single chromophore in a narrow polarity window.